

Drying of Asphalt Plant Aggregates Using Concentrated Solar Energy

M^a José Simón Castellano¹, Rubén Alexander López Quiroz¹, Sebastián Taramona¹,
Alessandro Gallo¹, Pedro Contreras- Lallana² and Jesús Gómez Hernández¹

¹ University Carlos III of Madrid, Department of Fluids and Thermal Engineering, Leganés (Spain)

² University Carlos III of Madrid, Department of Electronic Technology, Leganés (Spain)

Abstract

This experimental study investigates the feasibility of replacing rotatory kilns in hot mix asphalt plants with concentrating solar technology. A compound parabolic concentrator is used to focus solar irradiation onto a receiver where aggregates (silica sand in this study) are placed. The constant heat flux generated is employed to heat and dry the sand particles. Instruments such as thermocouples, pyranometers, a radiometer and a balance are employed to monitor temperature, solar irradiance, heat flux generated and humidity variations. The behavior of a 75 mm sand layer thickness is studied under several conditions of humidity and solar irradiation. Results are compared to different studies made under hot air-drying conditions. Temperature up to 70°C has been reached with a low concentration ratio technology, approximately 4 suns. Moreover, a 5 mm silica sand layer thickness has been dried in about 150 minutes.

Keywords: Hot Mix Asphalt plant; constant heat flux drying; Compound Parabolic Concentrator; silica sand; Solar heating technology.

1. Introduction

The most common material used in pavements is called Hot Mix Asphalt (HMA) which consists of a mixture of approximately 90% aggregates, 5% filler and 5% bitumen. The aggregates are heated up to a temperature between 150 and 200 °C. These temperatures are achieved in rotatory kilns, which are usually fueled with heavy fuel oil, natural gas, coal, etc. which are extremely polluting. In HMA plants rotary kilns consume around 85 kWh and cause the emission of 17.82 kg of CO₂ per metric ton of HMA produced (Peinado et al., 2011).

Decarbonization has become a key point in the current development of society and in reducing the effects of climate change. The inclusion of renewable energies is essential to meet the EU's climate change goals. For instance, Concentrating Solar Technologies (CST) are suitable for both electricity and heat generation for industrial processes. In this sense, linear Fresnel beam-down (LFBD) solar field can concentrate high irradiations on heavy receivers placed on the ground, opening a new technology path for drying and heating up of asphalt aggregates up to temperatures of 150 - 200 °C (Sánchez-González and Gómez-Hernández, 2020). To prove the feasibility of this process, a LFBD is currently under construction at Carlos III University of Madrid (UC3M) (Taramona et al., 2021a, 2021b). As a previous step in this research line, a less complex technology, such as a Compound Parabolic Concentrator (CPC) has been constructed and used at UC3M to obtain preliminary results. This study aims to experimentally test drying and heating processes of aggregates by means of a concentrated heat flux provided with the CPC.

Aggregates located in the receiving plane of the concentrator form a porous medium made up of silica sand particles, air and water. Drying a porous medium is a complicated process that involves simultaneous heat and mass transfer. Various mechanisms take place, such as conductive heat transfer due to the temperature rise, latent heat transfer necessary to generate water evaporation, vapor flow generated by differential pressure and water diffusion induced by capillary forces (Tang et al., 2018).

Several studies have analyzed mass and energy transfer on porous media with convection heats induced by hot air flows. In the study carried out by Tang et al. (2018) a theoretical model of convection drying of an unsaturated porous medium through a stream of hot air at different temperatures is analyzed. Lu et al. (2005) compared the development of a theoretical model with an experimental procedure also for drying a porous medium on a cylindrical wet bed with quartz particles. Min et al. (2019) investigated the aggregate layer drying by means of a

stream of hot air at different temperatures in a 4 mm layer thickness. This last study has been used as guidance for this work.

The present study consists of analyzing the effect of concentrated irradiance over a layer of aggregates (silica sand in this work) located in the focus of a CPC. To monitor the drying process, the irradiance on the receiver and the temperature rise, a high-precision balance, a radiometer and thermocouples placed in different regions of the sand layer are used, respectively. In addition, to determine the direct solar irradiation capture by the CPC, a couple of pyranometers and a shadow ring are used.

2. Experimental set up

The experimental study of the drying of aggregates using solar concentration technology is an innovative process for which there are no references. The study carried out by Min et al. (2019) analyzes the drying of silica sand by means of a stream of hot air. This material spatially arranged in a three-dimensional network forms quartz, the main component of common aggregates used in the construction sector or in industrial processes such as those carried out by HMA plants.

Silica sand has been used because of its chemical composition similarity with the aggregates used in the asphalt industry. However, since the size of the particles is not comparable with those used in asphalt plants, silica sand particles used in this work have been characterized.

Homogeneous particles are those whose shape, size and composition are practically identical; however, this is rarely the case. Therefore, through real sizes, a representative value of the set known as the equivalent or effective particle diameter is sought. Kunii and Levenspiel (1991) characterization process for intermediate size particles is followed to calculate this parameter. Sifting experiments are done and size particle distribution is obtained. Finally calculating mean particle diameter and making use of particle sphericity, effective particle diameter is obtained. Physical properties of used particles are collected in Tab. 1.

Tab. 1: Silica sand used physical properties.

| Parameter | Value |
|---|---------|
| Effective particle diameter, d_{eff} (μm) | 178.15 |
| Particle sphericity, ϕ_s (-) | 0.7-0.9 |
| Specific heat, C ($\text{J kg}^{-1} \text{K}^{-1}$) | 750.4 |
| Density, ρ (Kg m^{-3}) | 2660 |
| Thermal conductivity, k ($\text{Wm}^{-1}\text{K}^{-1}$) | 1.4 |

The heat flux needed to heat and dry aggregates is generated using the CPC prototype presented in Fig. 1. It redirects the incident solar rays from the lateral parabolas to the central flat area, where the receiver with the aggregates is located. It consists of a base structure made of aluminum profiles and four colorless methacrylate ribs to support and shape the lateral parabolas. Each parabola has been built using two 0.5 mm thick aluminum sheets adhered together. One for structural purposes and the other with a high reflectivity (0.85-0.95) surface to concentrate solar radiation.

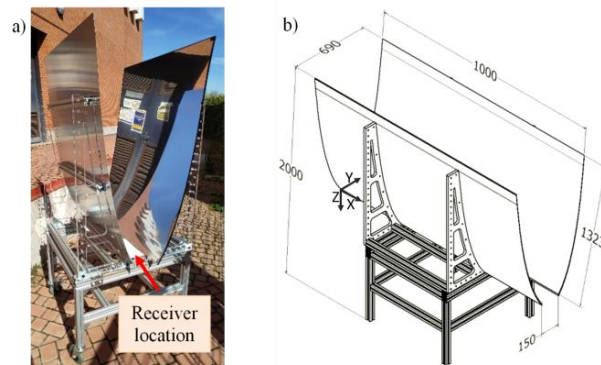


Fig. 1: (a) CPC prototype (b) CPC dimensions in mm.

The lateral parabolas are designed to redirect captured rays towards two focal lines causing a heterogeneous transversal distribution of irradiance concentration over the receiver plane where the top of the aggregates' receiver is placed. It can be seen in Fig. 2 where two brighter lines appear centered in the receiving plane over aggregates showing higher irradiation concentrations. Despite heterogeneous transversal distribution, longitudinal distribution can be assumed homogeneous. This will be considered to choose the thermocouples final positions.

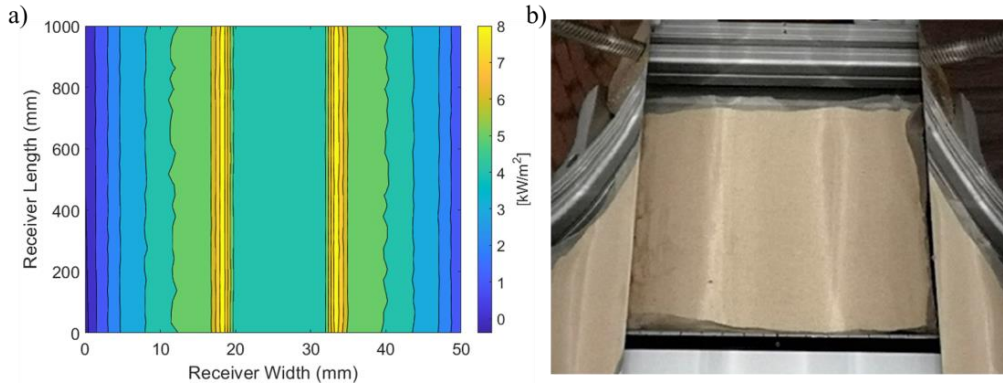


Fig. 2: Qualitative irradiance distribution on the receiver's surface: (a) ray tracing simulation, (b) experimental proceeding.

CPCs can harness both direct solar radiation and part of the diffuse radiation. The concentration capacity of this type of technology is defined by the geometric relationship between the area of the upper opening zone of the parabolas and the receiver plane area. The prototype used in these experimental proceedings has a 4.6 theoretical concentration ratio with an acceptance half-angle of 12.56 °. Maximum irradiances in the receiving plane will theoretically be 4.6 times the solar irradiance captured by the device.

$$C_i = \frac{A_{Aperture}}{A_{Receiver}} = 4,6 \text{ suns} \quad (\text{eq. 1})$$

The CPC is used to heat and dry aggregates. These must be placed in the receiver plane. Given the solar device dimensions and the need to place thermocouples to monitor the temperature evolution of the silica sand, a rectangular receiver has been designed and built meeting the desired specifications.

Some of the specifications considered to design the receiver are same width as CPC's receiver plane, sufficient height to study different sand layer thicknesses, full receiver total weight must be under maximum balance capacity, different thermocouples positions, high temperature resistant material and prevention of particle leakage.

Finally, in Fig. 3 the designed receiver is shown. It was optimized to feature a rectangular shape 150 mm wide, 200 mm long and 162 mm high. It is made up of two side plates, two front plates and a rectangular base made of 3 mm thick aluminum sheets.

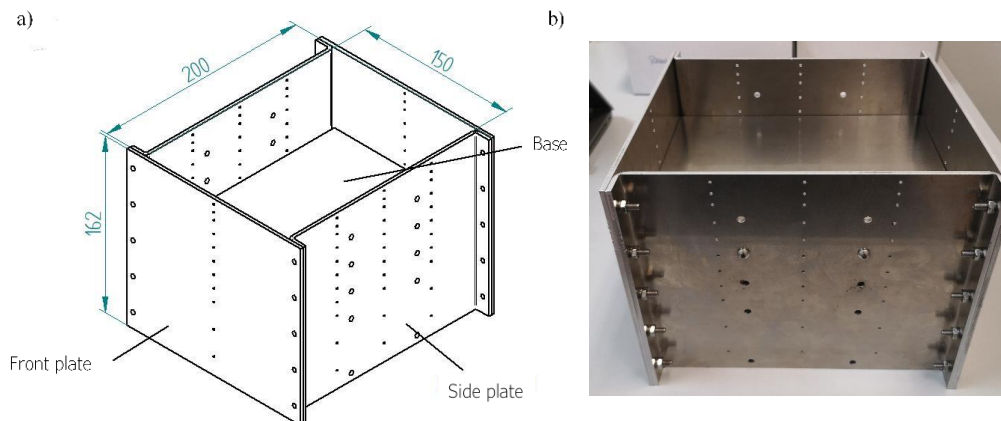


Fig. 3: Aggregates' receiver a) Design dimensions in mm, b) Real constructed design.

After preliminary tests it was found that one of the requirements was not met. There was particle leakage, so a small cell size metal mesh had to be introduced to meet all specifications described above.

Also, it was decided to set a fixed position for the base sheet. A thick sand layer would allow to know different silica sand layers behavior against the incident irradiance in the receiving plane at different exposure time. Furthermore, thermocouples positions were also fixed to determine heat diffusion inside the receiver depending on irradiance impinging on the receiver's surface. Final positions are shown in Fig. 4. Their coordinates are collected in Tab. 2.

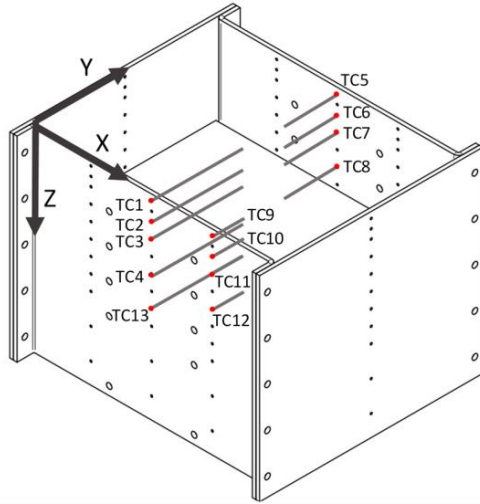


Fig. 4: Thermocouples' final positions.

Tab. 2: Thermocouples' final coordinates.

| Thermocouple | X (mm) | Y (mm) | Z (mm) |
|--------------|-----------|-----------|-----------|
| TC1 | 100 | 75 | 5 |
| TC2 | 100 | 75 | 20 |
| TC3 | 100 | 75 | 32.3 |
| TC4 | 100 | 75 | 57.3 |
| TC5 | 100 | 35 | 5 |
| TC6 | 100 | 35 | 20 |
| TC7 | 100 | 35 | 32.3 |
| TC8 | 100 | 35 | 57.3 |
| TC9 | 150 | 10 | 5 |
| TC10 | 150 | 10 | 20 |
| TC11 | 150 | 10 | 32.3 |
| TC12 | 150 | 10 | 57.3 |
| TC13 | 100 | 75 | 75 |

Instruments used to measure the variables of interest are two pyranometers, a radiometer, a high precision balance and thermocouples. The Hukseflux SR05-D1A3 and the Hukseflux SR15-D2A2 pyranometers measure respectively total and diffuse irradiance on the horizontal plane, while tests are taking place. The direct horizontal irradiance (DHI) on the ground is assessed by subtracting diffuse irradiance from total irradiance. Irradiance obtained with pyranometers have been compared daily with data provided by Aemet (<http://www.aemet.es/es/eltiempo/observacion/radiacion/radiacion?l=madrid>).

The concentrated irradiance over the receiver's plane is measured with a radiometer. It is placed in an aluminum sheet located in the center of the receiver's plane. The device used in this case is the SBG01 from Hukseflux. To monitor the mass loss due to water evaporation in drying tests the PS 10100.R2.M high precision balance from RADWAG is used. Finally, type-k thermocouples have been used to monitor the aggregates temperature evolution inside the receiver.

3. Methodology

Three kinds of experiments have been carried out: heating of aggregates without solar concentration, heating of aggregates with solar concentration and drying of aggregates by solar concentration. The difference between heating and drying tests is the aggregates' humidity content. In heating experiments silica sand does not contain water, while in drying a mass percentage of water is given to aggregates. These experiments show differences of using concentrating solar technologies for heating and the different transfer mechanisms that take place inside the aggregates.

Experiments took place in Leganés at Carlos III University of Madrid at Higher Polytechnic School campus. The location was chosen due to its proximity to the warehouse where facilities were stored, which coordinates are N 40° 20' 2'', W 3° 45' 53''. Tests were carried out between 11 a.m. and 3 p.m. in order to obtain a low cosine effect and achieve higher irradiation concentrations.

There are two main installations that must be prepared for these experiments, pyranometer's installation and the receiver with aggregates. The first one consists of a table where pyranometers and the shadow ring are anchored, Fig. 5. This installation allows an easy calibration for these devices that should be oriented after each test following their data sheet indications. The second installation depends on the performed test. In heating and drying experiments with solar concentration the receiver must be allocated inside the CPC while in heating process without solar concentration this receiver should be placed outside the CPC.



Fig. 5. Pyranometer's installation (left) and the CPC prototype used (right).

For concentrating solar experiments, temperature variation monitoring and CPC solar tracking to ensure azimuth alignment were carried out in 5 minutes intervals. Final concentrator position is achieved by visual shadow control generated by the structure itself. For the heating tests the aggregates exposure time has been 40 minutes. For the drying process exposure time has been between 90 and 180 minutes.

4. Results

CPC technology captures direct and part of diffuse solar irradiance. In all experiments, pyranometers measurements have been obtained and DHI was assessed. On sunny days, DHI reached values between 800 and 900 W/m^2 and the diffuse irradiance was lower than 200 W/m^2 . However, on cloudy days both barely exceeded 300 W/m^2 .

Irradiance concentrated on the receiver plane is measured with the radiometer. This value determines the incident heat flux on the center of the aggregates' receiver. On sunny days, it mainly depends on the direct irradiance received reaching almost 3800 W/m^2 while on cloudy days the heat flux obtained is significantly lower, not exceeding 1200 W/m^2 .

The relation between the irradiance measured with the radiometer at one arbitrary point of the receiver and the DHI shows a concentration factor of approximately 4 suns. This value is close to the estimated theoretical maximum value of 4.6. However, further analyses will be carried out to assess the concentrated irradiance distribution on the whole receiver plane.

Measured temperature shows different behaviors depending on which experiment has been performed. Heating tests without solar concentration show lower values than the ones performed with solar concentration for equal exposure time while drying tests tend to reach heating procedures temperatures after drying the sand layer.

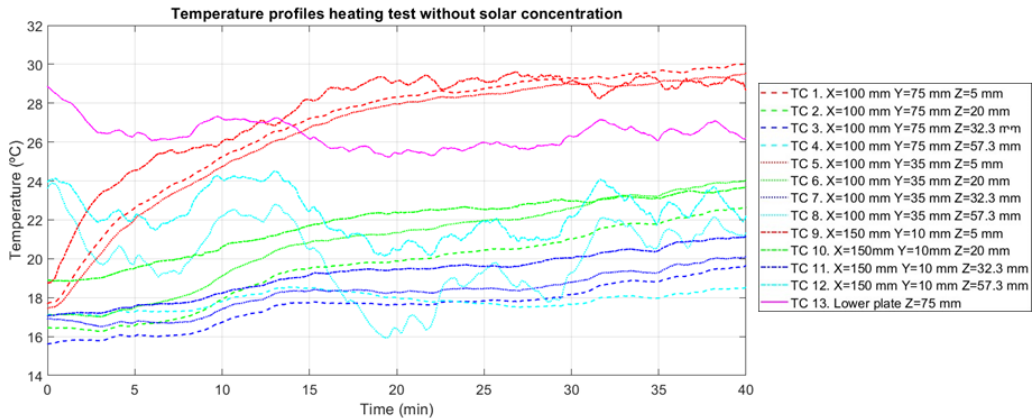


Fig. 6: Temperature profiles in a heating test without solar concentration for all thermocouples.

In Fig. 6 temperature evolution inside aggregates is shown for a heating test without solar concentration. Temperature profiles shown are grouped by color according to the corresponding thermocouple depth. Red color corresponds to thermocouples located 5 mm below the surface, the green ones 20 mm, blue for 32.3 mm, cyan for 57.3 mm and magenta for 75 mm depth, which corresponds to the lower plate thermocouple. In addition, they have been represented with different reliefs depending on Y position. The arrangement of the thermocouples in the transverse plane of the receiver for X = 100 mm and X = 150 mm is shown in Fig. 7 a and b.

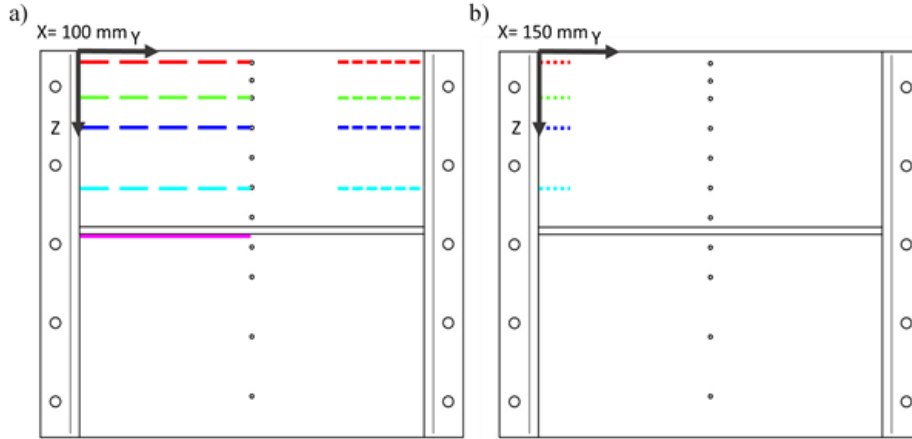


Fig. 7: Thermocouple color guide a) plane X = 100 mm, b) plane X = 150 mm.

Fig. 6 shows a temperature of the lower plate higher than the rest of the thermocouples at the beginning of the test. This is because of particle receiver is built with aluminum and it is exposed to solar irradiation without insulation, so its temperature increases. On the contrary, thermocouples introduced in the receiver have a lower temperature value because particles remain in the shade until they are introduced in the receiver to start the test.

This figure also shows how deepest thermocouples present high temperature values representing profiles similar to that obtained by the thermocouple located in the lower plate. Thermocouples represented in cyan do not show the temperature profile acquired by the particles when they are heated by solar irradiation, but they rather represent the temperature profile acquired by the particles by being in contact with the base.

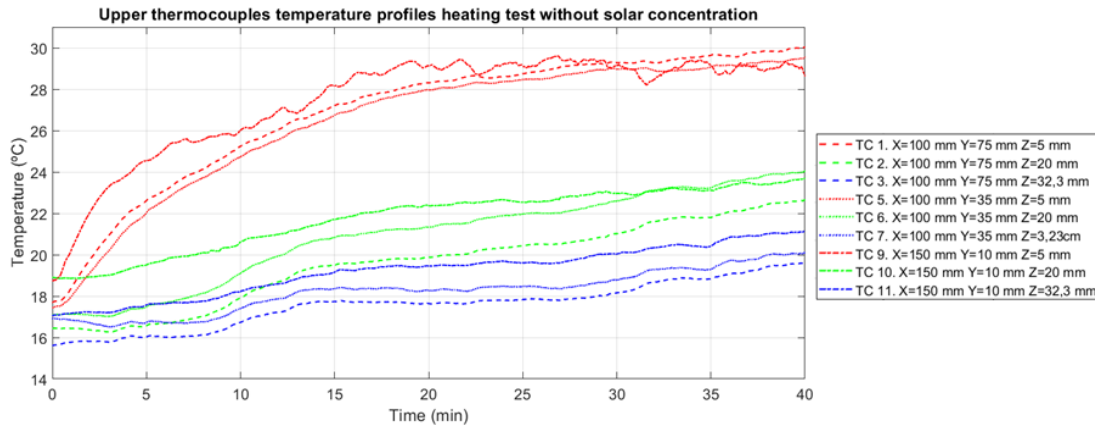


Fig. 8: Upper thermocouples temperature profiles in a heating test without solar concentration.

Fig. 8 shows the temperature profiles acquired by thermocouples due to the heat flux received by solar irradiation suppressing base and deepest thermocouples positions. As can be seen, they represent ascending temperature profiles where the upper layers reach higher temperatures at shorter times, stabilizing at the end of the experiment. The maximum temperature reached in this test without solar concentration was 30.83 °C in minute 40 of measurement.

It is worth noting the TC9 thermocouple fluctuating behavior, close to the surface. Controlling the thermocouples exact position is extremely difficult. In such small aggregate layer thicknesses, it is easy for one of them to be

misaligned getting closer to the surface. This is the reason why the TC9 thermocouple exhibits higher fluctuations. This presents a greater sensitivity to wind action, which increases convection losses and therefore temperature fluctuation.

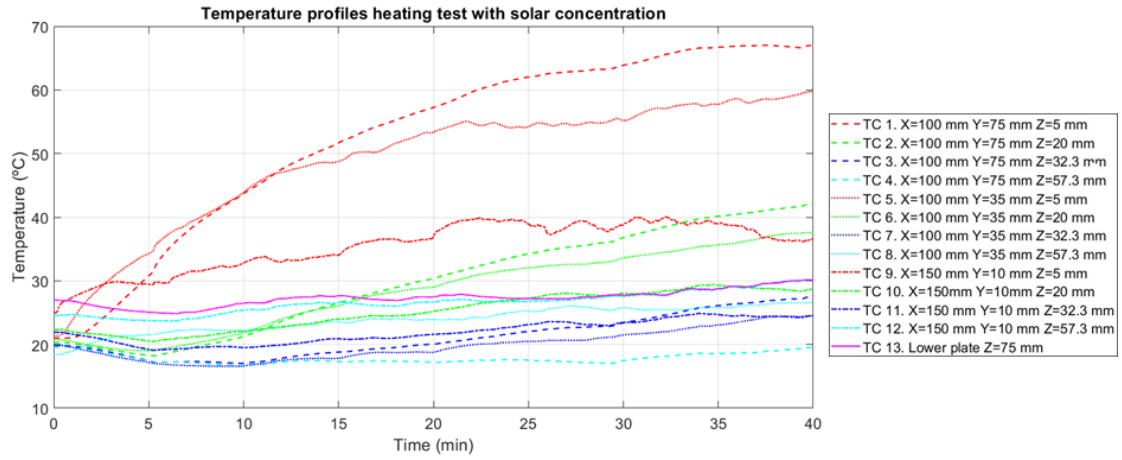


Fig. 9: Temperature profiles in a heating test with solar concentration.

Fig. 9 shows temperature profiles obtained by the thermocouples located inside the particles' receiver for a heating test using the CPC prototype. It can be observed how significantly higher temperatures are reached in comparison with those obtained without solar concentration technology. Maximum temperature reached is 75.70 °C in minute 40 by the TC1.

It should be noted that for each depth (Z), thermocouples located at greater Y, that is, in the central zone (Y = 75 mm), final temperature reached is higher than that obtained by thermocouples located at the same depth for lower Y values. Moreover, it can be seen inversely how lower Y values reach more rapidly a stabilization temperature. This effect demonstrates the dependence of stabilization and maximum temperature reached on incident irradiation concentration over receiver's surface.

A summary for all heating tests comparing TC1 thermocouple profiles is shown in Fig. 10. Profiles colored in blue represent aggregates heating obtained by solar concentration. Profiles shown in orange represent temperature profiles acquired by the aggregates in the absence of concentration.

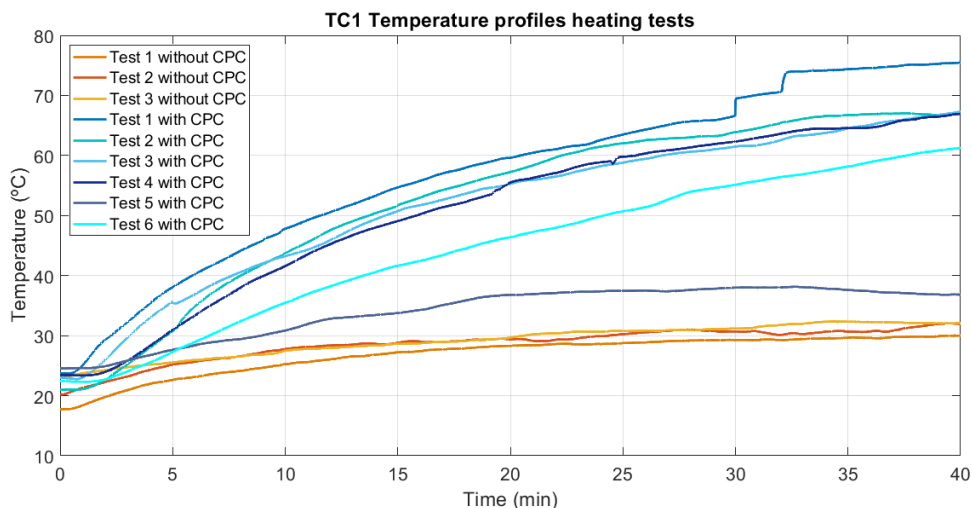


Fig. 10: TC1 temperature profiles in all heating experiments performed.

This graph compares the tests carried out with concentration and without solar concentration. Despite the meteorological dependence of this type of technology (Test 5), it can be observed the utility for favorable days. Making use of simple concentration technologies, as is the case of a CPC with a low concentration factor, 4 suns, temperatures above 70 °C could be reached.

Finally, drying experiments have been carried out. Moisture percentage present in aggregates used at asphalt industry ranges from 1-7% (Peinado et al., 2011). In these tests, different humidity percentages were analyzed to obtain different results. Mixtures with 5, 10 and 20% humidity were prepared.

Mixtures with higher water content did not show good cohesion. Water turned out to be filtered by the particles and lost by leaks in the receiver rather than by evaporation caused by irradiance concentration. 10% moisture mixtures did not present cohesion problems, but, nevertheless, they did not show remarkable results for the exposure time that took place during the tests. Finally, tests carried out with 5% humidity showed representative results.

The study carried out by Min et al. (2020) shows drying and heating temperature profiles obtained by thermocouples. Although in this study heat and mass transfer are produced by a stream of hot air, the behavior of the porous medium must be very similar. First, profiles would increase their temperature until reaching a stable value where evaporation would occur. Later, once the thickness reaches irreducible water saturation and the area can be considered dry, thermocouples increase their temperature again due to aggregates heating. Finally, temperature reached is stabilized at the air stream temperature used in each case. In the experiments carried out in this study, temperatures reached at the end of each test depend on the incident concentration flux on the receiver's surface.

In Fig. 11, the temperature profile acquired by the TC1 thermocouple shows the drying process in the initial phases described above. The initial stage of temperature increases and stabilizes due to upper layer moisture evaporation ($Z = 5$ mm). From minute 60 approximately, it is detected a perturbation in the slope associated with the end of evaporation process and the beginning of heating process.

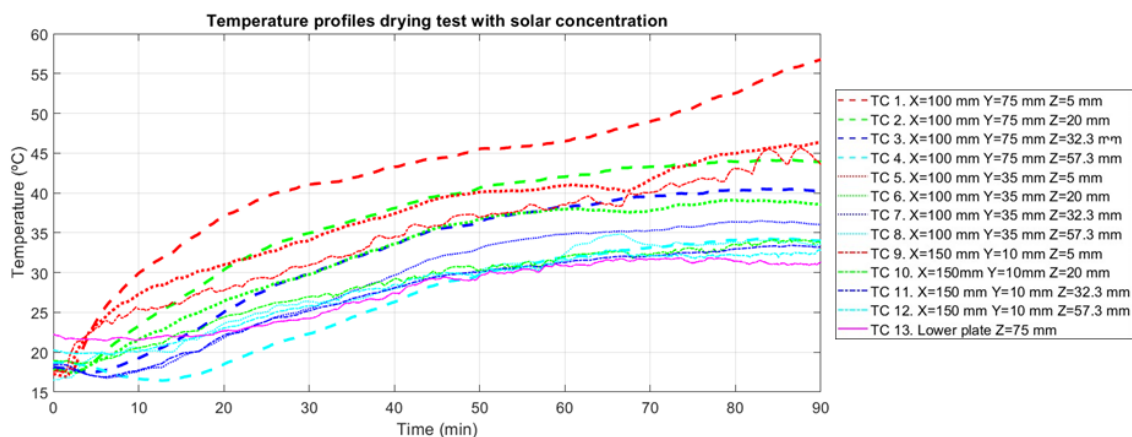


Fig. 11: Temperature profiles in a drying test with solar concentration.

Moreover, temperature in lower layers decreases its value at the beginning. Evaporation process requires large amounts of energy. In this case, it acquires it from deeper areas. The temperature reached is the wet bulb temperature. This is the one at which convection heat is offset by latent heat necessary for evaporation. The wet bulb temperature can be extracted from the psychrometric diagram where moist air properties, that in this case make up the porous medium, are exposed. The mixture introduced into the receiver is initially at a temperature of 18 °C, assuming an 80% air moisture content inside, wet bulb temperature reached is approximately 16 °C, value obtained in experimental tests.

Finally, a test that combined the previous ones was carried out, a drying and heating test. A mixture with 5% moisture water content has been exposed 180 minutes to solar irradiation concentration. Temperature profiles are shown in Fig. 12. This test also shows an initial temperature decrease for deeper thermocouples due to the energy input necessary for evaporation process. In the same way as in the previous test, if air temperature contained in aggregates at the beginning of the test is 18 °C and it is assumed that relative humidity is close to 80%, the wet bulb temperature that should be reached would be close to 16 °C, approximately the value obtained in the experiment.

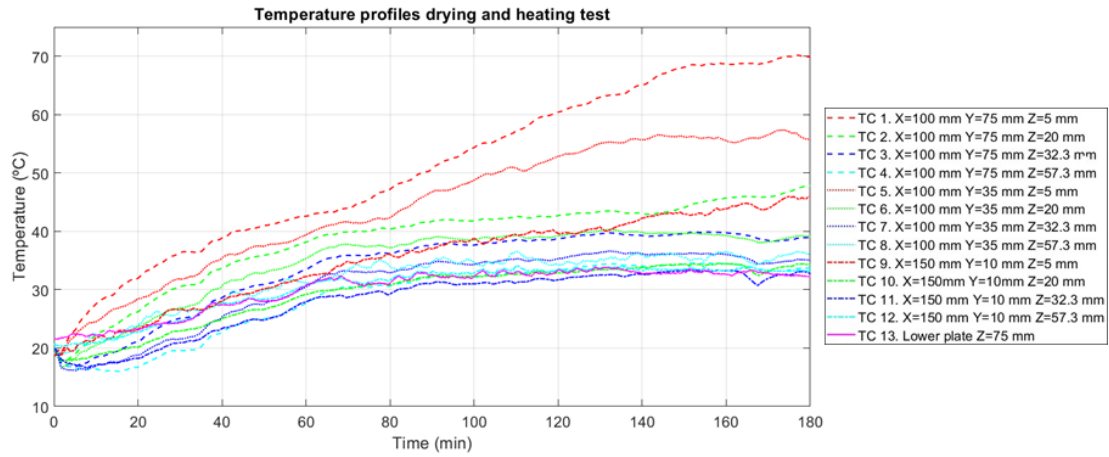


Fig. 12: Temperature profiles in the drying and heating test.

In addition, the stabilization and the slope change associated with the end of water evaporation can be observed for thermocouples located in the central zone of the receiver. This change takes place around minute 70 for thermocouple TC1, 80 for TC5, 135 for TC9, and 145 for thermocouple TC2. For the first two, it is also possible to observe the temperature stabilization due to heating, reaching 70.02 °C in the case of TC1. Thus, in Fig. 13, are collected drying temperature profiles for the entire 5 mm layer of aggregates colored in red, and the drying for the central thermocouple located at 20 mm in green. Black arrows indicate the end of the drying stage and the beginning of the heating one for each profile.

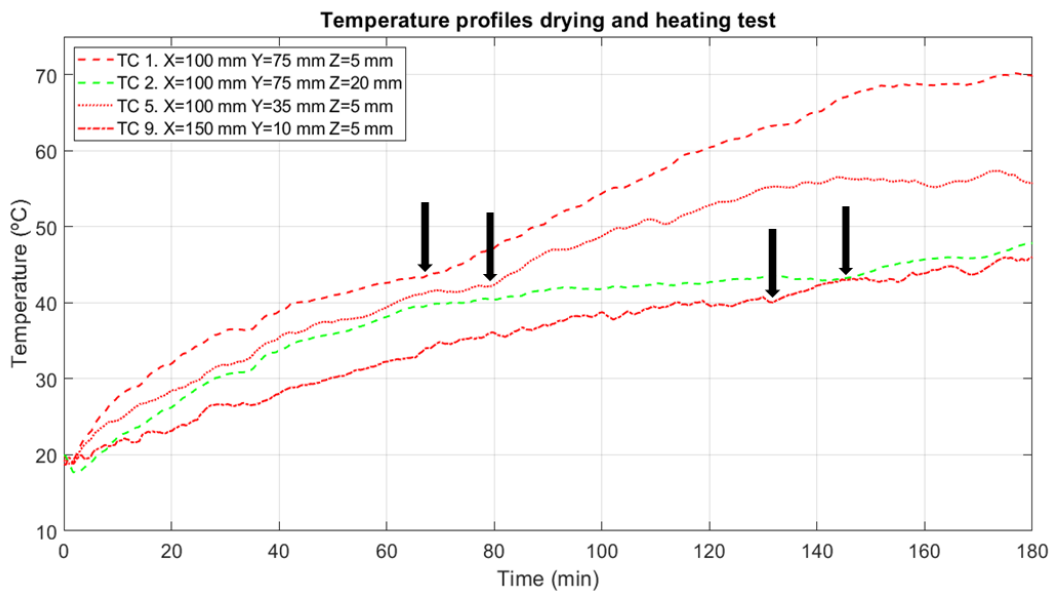


Fig. 13: Dried profiles at drying and heating test.

In drying tests, besides the observed temperature evolution inside the receiver, it is expected to know the moisture evaporation rate. Mass loss due to water evaporation during exposure time for the drying and heating test is shown in Fig. 14. This parameter is monitored by using a high precision balance. Several disturbances were collected due to experimental proceedings so that the signal obtained has been treated by means of a moving average digital filter. To carry out a detailed study, each of the disturbances and the trend between data blocks should have to be analyzed. In this work, given the time available, it is provided an approach analyzing the set trend for each trial. There were performed three drying tests and a drying and heating test with a 5% moisture content. The evaporation mass flows obtained are collected in Tab. 3.

Tab. 3: Evaporation mass flow drying 5% moisture content test.

| Drying test 5% moisture content | \dot{m}_{evap} (kg/s) | % \dot{m}_{evap} |
|---------------------------------|--------------------------------|---------------------------|
| 1 | $2.94 \cdot 10^{-6}$ | 0.0038 |
| 2 | $5.94 \cdot 10^{-6}$ | 0.0097 |
| 3 | $5.32 \cdot 10^{-6}$ | 0.0068 |
| Drying and heating test | $3.10 \cdot 10^{-6}$ | 0.0079 |

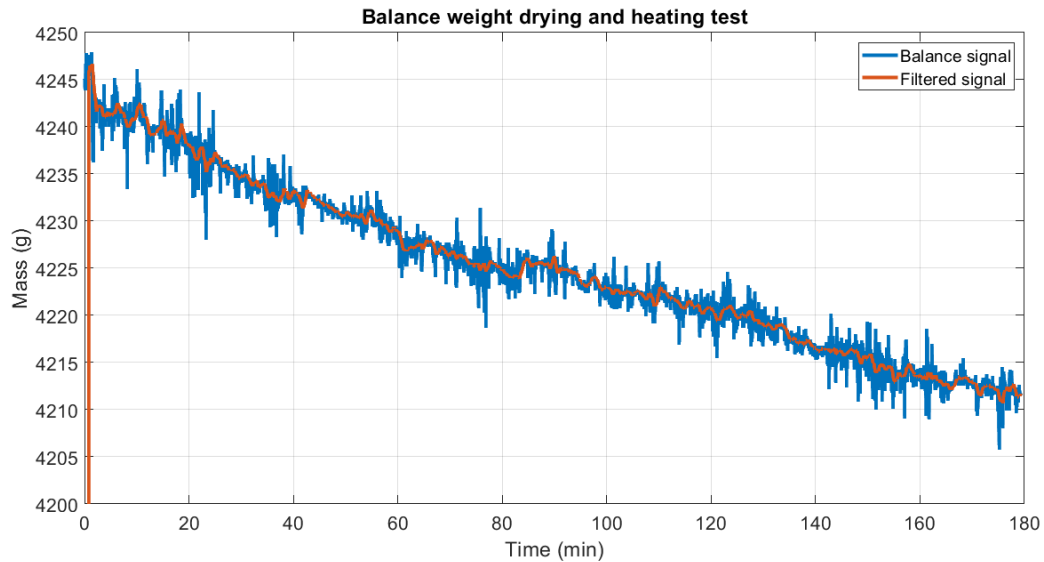


Fig. 14: Mass loss due to water evaporation at drying and heating test performed.

5. Conclusions

The main objective of this work was to obtain experimental results of aggregates drying by means of a concentrated heat flux. This is a fundamental and necessary step for the future integration of solar thermal technology in HMA plants. Thus, the study of heat and mass transfer mechanisms on a bed of silica sand, the main component of asphalt mixtures, has begun.

Results obtained show the effect of irradiance concentration on a porous medium. The temperatures reached within aggregates depend on the concentrated irradiance impinged on the receiver plane. It is demonstrated that for simple concentration technologies with low concentration capacities, approximately 4 suns, temperature of up to 70 °C can be reached.

In the drying tests, the evolution of temperature profiles inside aggregates has been compared with that obtained by Min et al. Short exposure times, 90 minutes, drying stages have been identified in different tests for a surface and centered area of the receiver. For long exposure times, 150 minutes, drying profiles have been obtained for the entire thickness of a 5 mm layer of silica sand.

Operating temperatures required by HMA production plants range between 150 and 200 °C. More complex solar concentration technologies, with higher concentration ratios (15-35 suns), as for example a linear-Fresnel beam down technology would allow the generation of higher heat fluxes and, therefore, provide higher temperatures. In addition, they would decrease the residence time in the receiver, which would imply a greater production of asphalt. For this purpose, a solar concentration prototype, based on the LFBF technology is currently being developed at Carlos III University of Madrid.

6. Acknowledges

The authors wish to thank the support for the research project INTECSOLARIS-CM-UC3M, funded by the call “Programa de apoyo a la realización de proyectos interdisciplinarios de I+D para jóvenes investigadores de la Universidad Carlos III de Madrid 2019-2020” under the frame of the “Convenio Plurianual Comunidad de Madrid - Universidad Carlos III de Madrid”.

The authors wish to thank “Comunidad de Madrid” for its support to the ACES2030-CM Project (S2018/EMT-4319) through the Program of R&D activities between research groups in Technologies 2018, co-financed by European Structural Funds.

7. References

Aemet <http://www.aemet.es/es/eltiempo/observacion/radiacion/radiacion?l=madrid> [Last Access Date: 14th October 2021]

Kunii, D., Levenspiel, O., 1991. Fluidization engineering. 2nd Ed. Butterworth-Heinemann. U.S.A.

Lu, T., Jiang, P., Shen, S., 2005. Numerical and experimental investigation of convective drying in unsaturated porous media with bound water. *Heat Mass Transf. und Stoffuebertragung* 41, 1103–1111. <https://doi.org/10.1007/s00231-005-0634-9>

Min, J.C., Zhang, Y., Tang, Y.C., 2020. Experimental study of wet porous sand layer air-drying characteristics. *Energy Reports* 6, 246–253. <https://doi.org/10.1016/j.egy.2019.08.052>

Peinado, D., De Vega, M., García-Hernando, N., Marugán-Cruz, C., 2011. Energy and exergy analysis in an asphalt plant’s rotary dryer. *Appl. Therm. Eng.* 31, 1039–1049. <https://doi.org/10.1016/j.applthermaleng.2010.11.029>

Sánchez-González, A., Gómez-Hernández, J., 2020. Beam-down linear Fresnel reflector: BDLFR. *Renew. Energy*. 146, 802-815. <https://doi.org/10.1016/j.renene.2019.07.017>

Tang, Y., Min, J., Wu, X., 2018. Selection of convective moisture transfer driving potential and its impacts upon porous plate air-drying characteristics. *Int. J. Heat Mass Transf.* 116, 371–376. <https://doi.org/10.1016/j.ijheatmasstransfer.2017.09.040>

Taramona, S., López-Quiroz, R.A., Gallo, A., Briongos, J.V., Gómez-Hernández, J. 2021a September 27 - October 01. Design and Construction of a Linear Beam-down Solar Field Demonstrator [Poster presentation]. SolarPACES2021. Online

Taramona, S., López-Quiroz, R.A., Gallo, A., Gómez-Hernández, J. 2021b, October 04-06. Prototype design and first tests of a linear beam-down solar field [Paper presentation]. International Conference on Polygeneration. Online.